

# Structural and Photoluminescent Studies of $\text{Eu}^{3+}$ -Doped $\text{Sr}_2\text{SiO}_4$ Phosphor

M Somani<sup>1</sup>, M Saleem<sup>2\*</sup> , M Mittal<sup>1</sup> and P K Sharma<sup>1</sup>

<sup>1</sup>Department of Physics, Government Autonomous Holkar Science College, Indore 452001, India

<sup>2</sup>Materials Science Laboratory, School of Physics, Vigyan Bhawan, Devi Ahilya University, Khandwa Road Campus, Indore 452001, India

Received: 07 September 2018 / Accepted: 23 July 2019 / Published online: 5 October 2019

**Abstract:** Here, we report the synthesis of  $\text{Sr}_{2-x}\text{Eu}_x\text{SiO}_4$  ( $\text{Sr}_2\text{SiO}_4:\text{Eu}^{3+}$ ) [ $x = 0.01, 0.015, 0.02, 0.025, 0.03$ ] silicate phosphors via high-temperature solid-state reaction method. The prepared phosphors were X-ray diffraction (XRD) characterized, and the analysis of XRD data conveyed that all the samples are crystalline, single-phased and have crystallized to orthorhombic structure (*Pmnb*). The structure, space group (*Pmnb*) and other structure concerned parameters were further verified using Rietveld refinement for  $x = 0.01$  phosphor. The XRD pattern for all the synthesized phosphors was identical in appearance, and there is no evidence of the new peak with increased doping of  $\text{Eu}^{3+}$  ion. This behavior may be attributed to the uniform distribution of rare earth  $\text{Eu}^{3+}$  ion at  $\text{Sr}^{2+}$  site due to comparative ionic size of the host and guest ion. The formation of  $\text{Sr}_2\text{SiO}_4:\text{Eu}^{3+}$  phosphors is verified further by FTIR spectroscopic technique. To investigate optical band gap of prepared phosphors, UV–Vis diffuse reflectance spectroscopic studies have been carried out. Photoluminescence property of  $\text{Sr}_2\text{SiO}_4:\text{Eu}^{3+}$  phosphors was studied. The emission spectrum displayed characteristic emission peaks corresponding to  $\text{Eu}^{3+}$  around 587, 612 and 702 nm. The Commission International de l’Eclairage color coordinates were found lying in orange-red region.

**Keywords:** XRD; Phosphor; Photoluminescence; CIE coordinates

**PACS Nos.:** 81.20-n; 61.05.cp; 78.20-e; 78.30–j

## 1. Introduction

Solid-state lighting by means of LEDs based on the  $\text{Sr}_2\text{SiO}_4$  phosphors has attracted researchers because of their excellent performance such as high energy efficiency, and environmental protection. Light emitting diodes (LEDs) with their characteristics of high brightness, reliability, long life time, low environmental impact and energy efficiency are expected to replace conventional incandescent and fluorescent lamps in the near future. They exhibit easy, cost-effective and convenient manufacturing technology that guarantees their dominating nature in LED market. In addition to this, they are beneficial in terms of low production cost, possess high chemical and physical stability, have corrosion-resistant nature and are thermally stable [1, 2].  $\text{M}_2\text{SiO}_4:\text{Eu}$  ( $\text{M} = \text{Ca}, \text{Sr}, \text{Ba}$ ) phosphors have

attracted serious concentration of the phosphor community after the invention of white light emitting diodes (LEDs). The first  $\text{Eu}^{2+}$ -activated luminescence in alkaline earth orthosilicate phosphor was reported in 1968. ( $\text{Ca}, \text{Sr}, \text{Ba}$ ) $_2\text{SiO}_4:\text{Eu}$  orthosilicate phosphors are excellent commercial phosphors for white LEDs as they exhibit high light conversion efficiency for near ultraviolet (NUV) and blue light [3].

$\text{M}(\text{M} = \text{Ca}, \text{Sr}, \text{Ba})_2\text{SiO}_4:\text{Eu}$  can produce more colorful emission of the white LEDs with lower colors and higher colors [4, 5] as per the requirement that depends upon the dopants, the process of manufacturing and the conditions. The commercial  $\text{M}_2\text{SiO}_4:\text{Eu}^{3+}$  phosphors are mostly produced by high-temperature solid-state reaction method as it provides high light conversion efficiency. This synthesis method requires high firing temperature and introduction of flux to promote crystallization giving rise to growth in particle size, wide particle distribution and asymmetric morphology. However, from the context of application, the

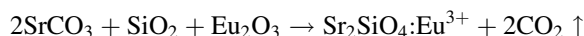
\*Corresponding author, E-mail: mscphy7@gmail.com

phosphors for LEDs must possess suitable average crystallite size ( $< 10 \mu\text{m}$ ) and narrow distribution of particles to achieve high brightness and considerable color coordinates [6, 7].

In this report, the orthosilicates of the type  $\text{Sr}_{2-x}\text{Eu}_x\text{SiO}_4$  [ $x = 0.01, 0.015, 0.02, 0.025, 0.03$ ] synthesized via solid-state reaction route are reported. These phosphors were characterized for structural studies via XRD and FTIR techniques. For optical properties, UV-Vis and PL spectral studies were carried out.

## 2. Experimental details

The orthosilicates phosphors with general formula  $\text{Sr}_{2-x}\text{Eu}_x\text{SiO}_4$  [ $x = 0.01, 0.015, 0.02, 0.025, 0.03$ ] were synthesized by high-temperature solid-state reaction (SSR) method. The starting materials  $\text{SrCO}_3$ ,  $\text{SiO}_2$  and  $\text{Eu}_2\text{O}_3$  were of analytic grade and highly pure. For  $x = 0.01$ ,  $\text{Sr}_{2-x}\text{Eu}_x\text{SiO}_4$  phosphor, stoichiometric amount of these starting materials was thoroughly mixed in agate mortar for 2 h [8]. The powdered mixture was calcined at  $1050^\circ\text{C}$  for 4 h. The obtained mixture was again ground for 2 h and was annealed at  $600^\circ\text{C}$  for 3 h. The product was finally ground until fine powder was obtained and converted into the pellets of the diameter of 10 mm at a pressure of 10 tonnes/inch. All other phosphors were synthesized by the same procedure. The chemical reaction used for stoichiometric calculation is:



The structural characterization, i.e., the confirmation of type of phase and crystal structure, of the as-prepared phosphors was carried out by X-ray diffraction using a Bruker D8 advanced X-ray diffractometer. The data were collected over the angular range,  $10^\circ < 2\theta < 80^\circ$  with a step size of 0.02. FTIR spectra were recorded with the help of Frontier-Perkin-Elmer FTIR SP 10 STD for investigation of the fingerprint region ( $400\text{--}1400 \text{ cm}^{-1}$ ) as well as the functional group region ( $1400\text{--}4000 \text{ cm}^{-1}$ ) of  $\text{Sr}_2\text{SiO}_4:\text{Eu}^{3+}$  phosphors by mixing the sample with potassium bromide (KBr). UV-Vis spectrometer (Perkin Elmer, Lambda 950—USA) was used to obtain the spectroscopic data to be analyzed for the band gap of the samples under investigation. Photoluminescence measurements were carried out using an Edinburgh Instrument FLS920-s fluorescence spectrometer. All the characterizations were carried out at room temperature.

## 3. Results and discussion

### 3.1. Structural analysis

The highly crystalline  $\text{Sr}_{2-x}\text{Eu}_x\text{SiO}_4$  ( $\text{Sr}_2\text{SiO}_4:\text{Eu}^{3+}$ ) [ $x = 0.01, 0.015, 0.02, 0.025, 0.03$ ] silicate phosphors synthesized were XRD-characterized for the confirmation of phase formation and the crystal structure. Figure 1(a) shows the X-ray diffraction patterns of  $\text{Sr}_2\text{SiO}_4:\text{Eu}^{3+}$  phosphors. The analysis of XRD spectra of the synthesized  $\text{Sr}_2\text{SiO}_4:\text{Eu}^{3+}$  phosphors revealed that all the prepared samples have crystallized into the single-phased orthorhombic structure ( $Pmnb$ ) without any trace of secondary phase within the experimental limits and over the entire  $\text{Eu}^{3+}$  ion concentration. The XRD spectra of the reported samples match well with the JCPDS card [JCPDS 32-1256] [9]. All diffraction patterns were collected at room temperature.

The average crystallite size of the  $\text{Sr}_2\text{SiO}_4:\text{Eu}^{3+}$  phosphor was calculated to be 27–40 nm range using Scherer formula [10–12],  $t = k\lambda/\beta\cos\theta$ , where ‘ $t$ ’ is average crystallite size,  $k$  ( $= 0.9$ ) is shape factor,  $\beta$  is the FWHM of the characteristic peak, and  $\theta$  is the diffraction angles. To

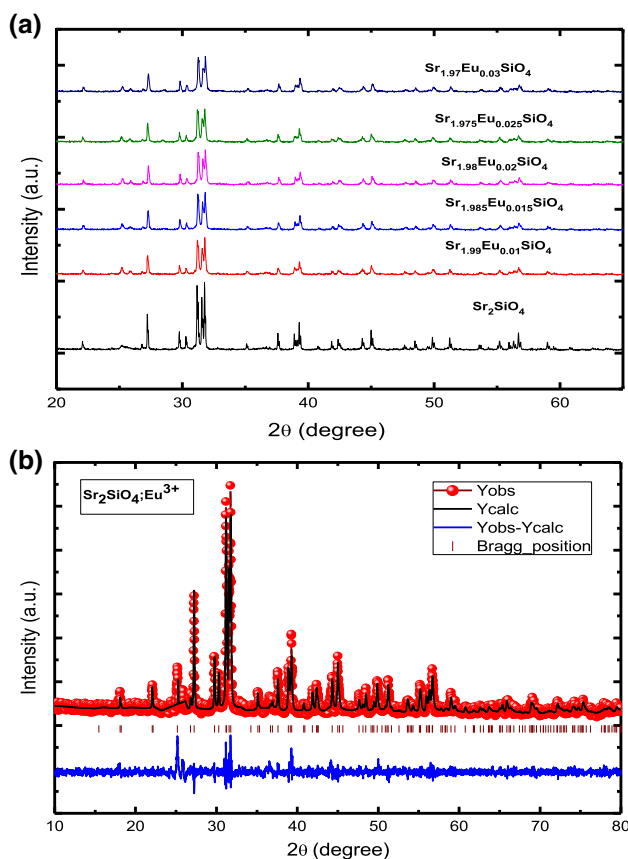


**Fig. 1** (a) XRD patterns of  $\text{Sr}_{2-x}\text{Eu}_x\text{SiO}_4$  [ $x = 0.01, 0.015, 0.02, 0.025, 0.03$ ] and (b) Rietveld refinement of  $\text{Sr}_{1.9}\text{Eu}_{0.01}\text{SiO}_4:\text{Eu}^{3+}$  silicate phosphors

verify the crystal structure, type of phase, and other structure-related parameters, only the XRD data of  $\text{Sr}_{2-x}\text{Eu}_x\text{SiO}_4$  [ $x = 0.01$ ] silicate phosphor were Rietveld-refined as all others are identical to it. The refinement is shown in Fig. 1(b), and a close investigation reveals that all the reflection peaks are refined and there is no extra peak in the limits of the experiment. This behavior is examined for the XRD patterns of all the phosphors with varied concentrations of  $\text{Eu}^{3+}$  ion. The well matching of the XRD spectra and the absence of new reflection peaks convey uniform distribution of  $\text{Eu}^{3+}$  ion at the  $\text{Sr}^{2+}$  ion site of the host. This is attributed to the nearly equal ionic size of  $\text{Eu}^{3+}$  ion and  $\text{Sr}^{2+}$  ion. Figure 2 shows the crystal structure of  $\text{Sr}_{2-x}\text{Eu}_x\text{SiO}_4$  [ $x = 0.01$ ] silicate phosphor. The various structural parameters calculated via refinement are summarized in Table 1.

### 3.2. Composition and morphology

To study the luminescence of the  $\text{Sr}_{1.99}\text{Eu}_{0.01}\text{SiO}_4$  phosphor, it is necessary to confirm the composition of the sample as the physical properties are highly dependent on the dopants and their concentration. Therefore, we carried out the energy-dispersive analysis of the X-rays (EDAX) characterization. The EDAX spectrum for  $\text{Sr}_{1.99}\text{Eu}_{0.01}\text{SiO}_4$  phosphor is shown in Fig. 3. The spectrum reveals the presence of the all the constituents of the prepared sample without loss of any integral element within the bounds of the experiment. This compositional verification allows to study the other physical properties and hence the effect of doping.

In addition to the necessity of composition in studying physical properties of the as-prepared phosphors, the

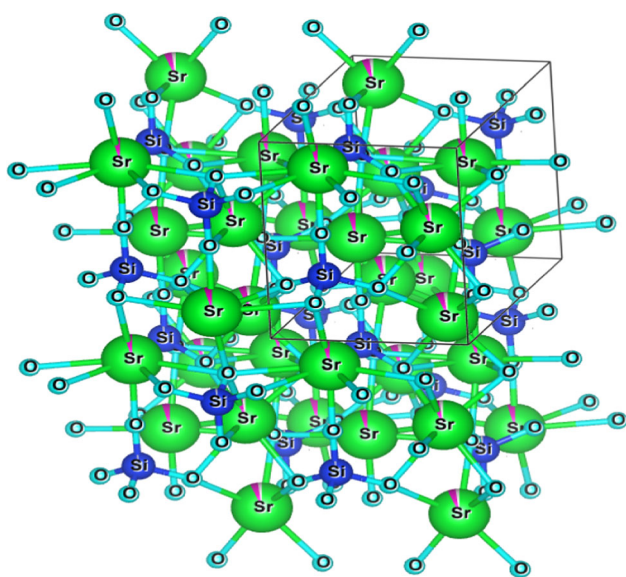


Fig. 2 Crystal structure of pristine  $\text{Sr}_2\text{SiO}_4$  orthosilicate

Table 1 Details of Rietveld-refined XRD pattern of the  $\text{Sr}_{1.99}\text{Eu}_{0.01}\text{SiO}_4$  orthosilicate phosphor

S. no.	Parameters	Obtained values
1	Space group	<i>Pmmn</i>
2	<i>a</i> (Å)	5.6654
3	<i>b</i> (Å)	7.0737
4	<i>c</i> (Å)	9.7336
5	<i>V</i> (Å <sup>3</sup> )	390.0778
6	Density	4.634 g/cm <sup>3</sup>
7	<i>R<sub>F</sub></i>	6.19
8	<i>R<sub>Bragg</sub></i>	9.14
9	<i>R<sub>wp</sub></i>	34.2
10	<i>R<sub>exp</sub></i>	25.6
11	<i>R<sub>p</sub></i>	37.9
12	$\chi^2$	1.731
13	GOF	1.3

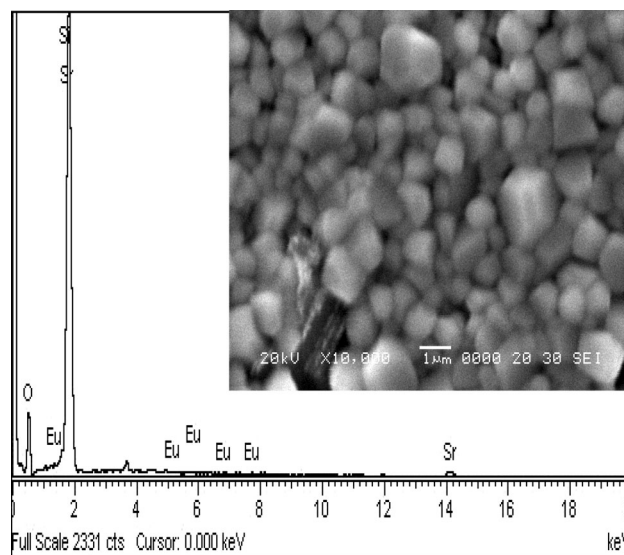


Fig. 3 EDAX and SEM (inset) of  $\text{Sr}_{1.9}\text{Eu}_{0.01}\text{SiO}_4:\text{Eu}^{3+}$  silicate phosphors

morphology study is of immense importance. The morphological study has been carried out employing scanning electron microscopy (SEM). The SEM image obtained is shown as an inset in Fig. 3. The analysis of the micrograph reveals that sample has well-grown grains as a result of high-temperature treatment [13]. However, there is no clear grain boundary between the grains so obtained. Meanwhile, one cannot comment that the sample is porous in nature. Regarding the compactness in the sample, the sample exhibits intermediate character which allows the movement of the charges from their mean positions to the excited ones where they are trapped by the traps created via doping and hence shows the phenomenon of luminescence. The grain

size was estimated using ImageJ software which revealed the average size of the grains lies in the range of 1.25–2  $\mu\text{m}$  which is suitable for the phosphor for application in the luminescence-based devices. Further, from the SEM micrograph the particles appear to be uniformly distributed throughout as required.

### 3.3. Fourier transform infrared spectroscopy

The Fourier transform infrared spectrum has been widely used for identification of organic and inorganic compounds. The FTIR spectrum of  $\text{Sr}_{2-x}\text{Eu}_x\text{SiO}_4$  [ $x = 0.01, 0.015, 0.02, 0.025, 0.03$ ] silicate phosphors is displayed in Fig. 4. The vibrational mode corresponding to Si–O stretching [ $F_2$  ( $\gamma_3$ )] appears at the range of 800–970  $\text{cm}^{-1}$ . The Sr–O stretching vibration is represented by the characteristic absorption band appearing at 1470  $\text{cm}^{-1}$ . The absorption bands observed in the range of 1900–1700  $\text{cm}^{-1}$  are asymmetric stretching of ( $\text{CO}_3^{2-}$ ) carbonates [14, 15]. The fingerprint vibrations of  $\text{SiO}_2$  correspond to the wave numbers 775 and 855  $\text{cm}^{-1}$  [16]. FTIR spectra for all the concentrations of the  $\text{Eu}^{3+}$  rare earth ion are identical, and hardly any mentionable change is observed. This again validates the discussion on the XRD that  $\text{Eu}^{3+}$  is uniformly distributed at  $\text{Sr}^{2+}$  site of the host and that all the samples are monophasic in nature.

### 3.4. UV–Vis spectroscopy

The UV–Vis diffuse reflectance spectroscopic measurements were carried out to investigate the optical energy band gap of synthesized  $\text{Sr}_{2-x}\text{Eu}_x\text{SiO}_4$  [ $x = 0.01, 0.015, 0.02, 0.025, 0.03$ ] silicate phosphors. Figure 5 shows the UV–Visible spectrum of the phosphors prepared. To

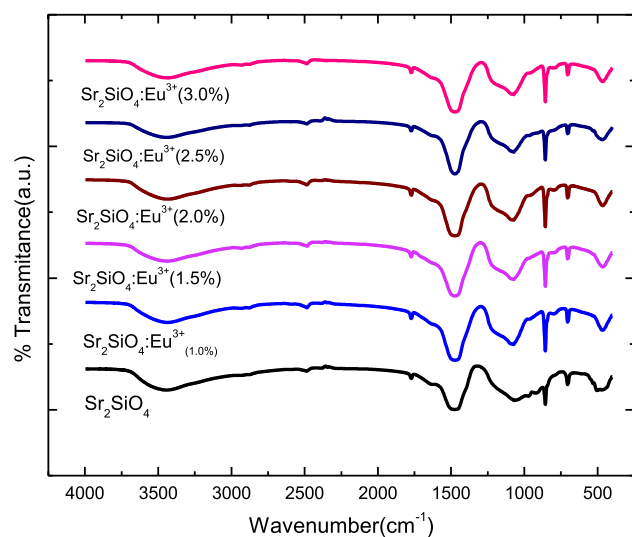


Fig. 4 FTIR spectrum of  $\text{Sr}_2\text{SiO}_4:\text{Eu}^{3+}$  phosphors

determine the optical band gap energy of  $\text{Sr}_{2-x}\text{Eu}_x\text{SiO}_4$  [ $x = 0.01, 0.015, 0.02, 0.025, 0.03$ ] silicate phosphors, we used Tauc relation written in the form of Kubelka–Munk function [17]. The band gap was estimated by plotting the square of the Kubelka–Munk function  $F(R) = (1 - R)^2/2R$  where  $R$  is reflectance and  $n$  is transition-dependent integer [17] against the energy ( $h\nu$ ). In the present case, we obtained the best fit by plotting  $[h\nu F(R)]^n$  against  $h\nu$  for  $n = 2$ , i.e., allowed indirect transition. The optical band gap value of  $\text{Eu}^{3+}$ -doped  $\text{Sr}_2\text{SiO}_4$  phosphors was obtained by extrapolating a straight line along the sharp edge of the curve that cuts the energy axis at certain point. The intercept made by extrapolated line on the energy axis is the estimation of energy band gap value. The band gap values of all the synthesized phosphors are observed initially to increase up to the  $\text{Eu}^{3+}$  concentration  $x = 0.02$  and then decline with the further increase in concentration of  $\text{Eu}^{3+}$ . This is indicative of the increase in emission spectra in the initial which is maximum for  $\text{Eu}^{3+}$  ion concentration,  $x = 0.02$ , and then decreases gradually and agrees with the report elsewhere [18].

### 3.5. Photoluminescence

The optical properties of  $\text{Sr}_{2-x}\text{SiO}_4:x\text{Eu}^{3+}$  ( $x = 0.01, 0.015, 0.02, 0.025, 0.03$ ) silicate phosphors, for the excitation and emission spectra was recorded at room temperature displayed as concentration dependence in Figs. 6 and 7 using radiation of 394 nm. The excitation spectrum of the as-prepared samples for the 612 nm emission is shown in Fig. 6.  $\text{Eu}^{3+}$  ion emits a characteristic red light with several lines due to the  $4f-4f$  ( ${}^5\text{D}_0 \rightarrow {}^7\text{F}_j$ ) transitions ( $J = 0, 1, 2, 3, 4$ ). From the excitation plot, it is clear that the strongest sharp peak appears at 394 nm which is attributed to the  ${}^7\text{F}_0 \rightarrow {}^5\text{L}_6$  transition of  $\text{Eu}^{3+}$ . In addition to this characteristic transition peak, the less intense excitation peaks located at 319 nm, 362 nm and 386 nm are ascribed to intra-configurational  $4f-4f$  transitions which are forbidden as well as hypersensitive transitions of  $\text{Eu}^{3+}$  ion. These transitions can be assigned to  ${}^7\text{F}_0 \rightarrow {}^5\text{H}_6$ ,  ${}^7\text{F}_0 \rightarrow {}^5\text{D}_4$  and  ${}^7\text{F}_0 \rightarrow {}^5\text{G}_4$  transitions, respectively.

The emission spectra of  $\text{Sr}_2\text{SiO}_4:\text{Eu}^{3+}$  phosphor displayed in Fig. 7 for the excitation of 394 nm were recorded in the range of 450–750 nm. The emission transitions are observed comprising a series of sharp emission peaks due to excited state  ${}^5\text{D}_0$  to the ground state  ${}^7\text{F}_j$  (where  $j = 0, 1, 2, 3, 4$ ) transitions. The emission transition  ${}^5\text{D}_0 \rightarrow {}^7\text{F}_1$  at 587 nm (orange region) is assigned to magnetic dipole. The strongest emission peak at 612 nm (red region) is assigned to electric dipole. Also the emission at 651 nm is attributed to  ${}^5\text{D}_0 \rightarrow {}^7\text{F}_3$  transition. Similarly, the emission at 702 nm is attributed to  ${}^5\text{D}_0 \rightarrow {}^7\text{F}_4$  transition [18]. Due to the little

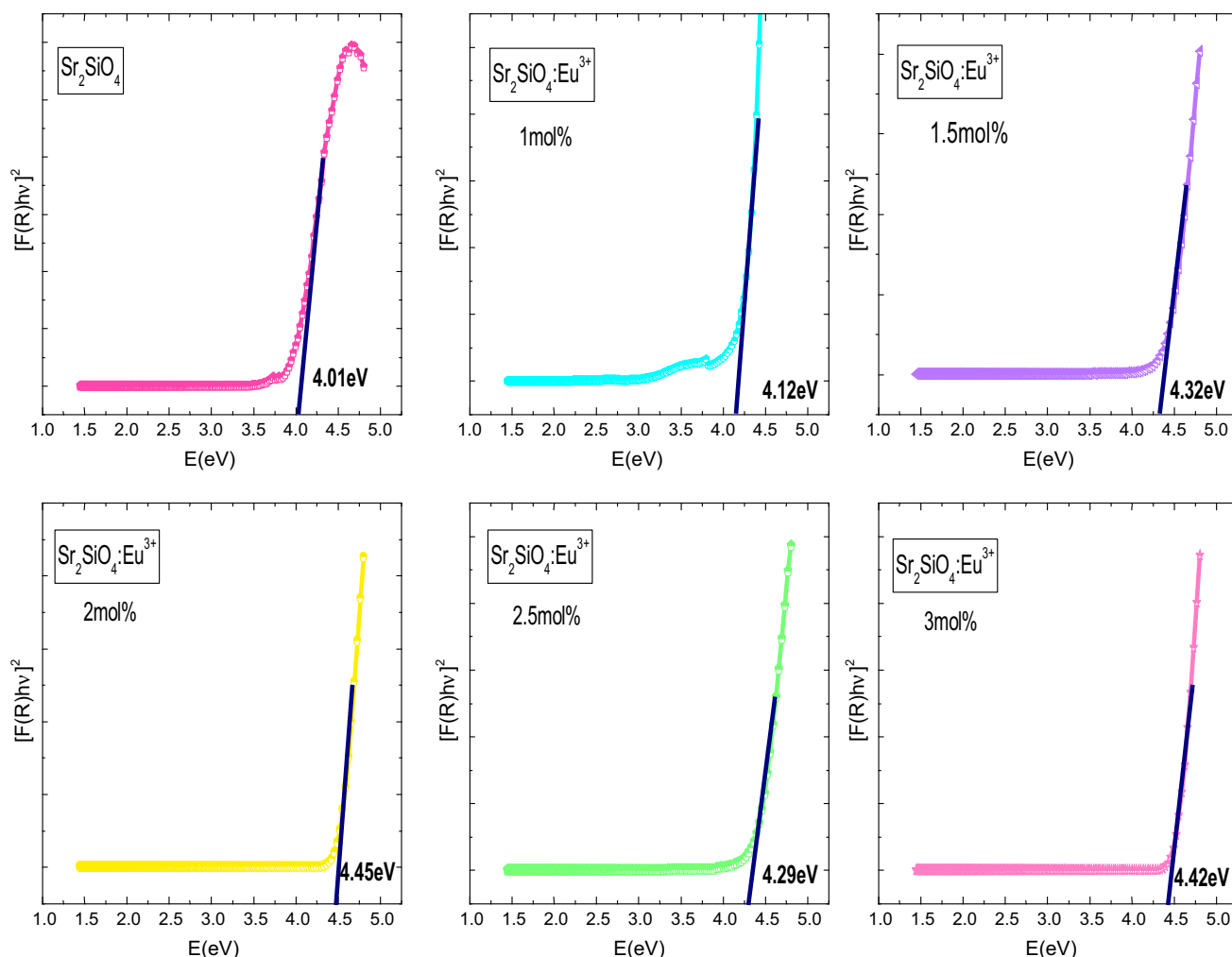


**Fig. 5** UV Visible plots of  $\text{Sr}_2\text{SiO}_4:\text{Eu}^{3+}$  phosphors

difference between ionic sizes of  $\text{Eu}^{3+}$  and  $\text{Sr}^{2+}$ , we presume that the  $\text{Eu}^{3+}$  ion replaces  $\text{Sr}^{2+}$  ion site and hence this emission at 587 and 612 nm does exist [19].

The emission intensity increases with the increase in  $\text{Eu}^{3+}$  concentration from  $x = 0.01$  to  $x = 0.02$ , and afterward, it decreases with further increase in the concentration of  $\text{Eu}^{3+}$  ions attributed to the concentration quenching process. Thus, from the emission spectra, we have observed that  $x = 0.02$  is the optimized concentration. The increase in PL emission intensity observed may be due to the decrease in cross-relaxation between  $\text{Eu}^{3+}$  ions.

The concentration quenching might be due to non-radiative energy transfer from one  $\text{Eu}^{3+}$  to other  $\text{Eu}^{3+}$  ion, which can be divided into two mechanism viz. (1) multipole–multipole interaction and (2) Dexter mechanism or exchange interaction. The energy transfer mechanism in phosphor is essential to obtain the critical transfer distance ( $R_c$ ). Blessed [20] proposed the critical transfer distance

( $R_c$ ) which can be estimated by the critical concentration of activator ion ( $\text{Eu}^{3+}$ ) using the relation

$$R_c = 2 \left[ \frac{3V}{4x_c N} \right]^{1/3} \quad (1)$$

where  $x_c$  is the critical concentration of  $\text{Eu}^{3+}$  ion,  $N$  is the number of cations in the unit cell, and  $V$  is the volume of the unit cell. For  $\text{Sr}_2\text{SiO}_4:\text{Eu}^{3+}$  phosphors, the volume of the unit cell is  $\approx 390.077 \text{ \AA}^3$  and the critical concentration which results from maximum intensity of  $\text{Sr}_{2-x}\text{Eu}_x\text{SiO}_4$  phosphor is  $x_c = 0.02$ . In addition, the number of host cations in the unit cell is 8. Using all the parameters, the estimated critical distance of energy transfer  $R_c$  calculated using Eq. (1) was found to be  $16.7 \text{ \AA}$ . The energy interaction mechanism was only possible when critical energy transfer distance  $\approx 5 \text{ \AA}$ , which is very less than the calculated result; hence, it indicates that the exchange interaction mechanism was ineffective in energy transfer

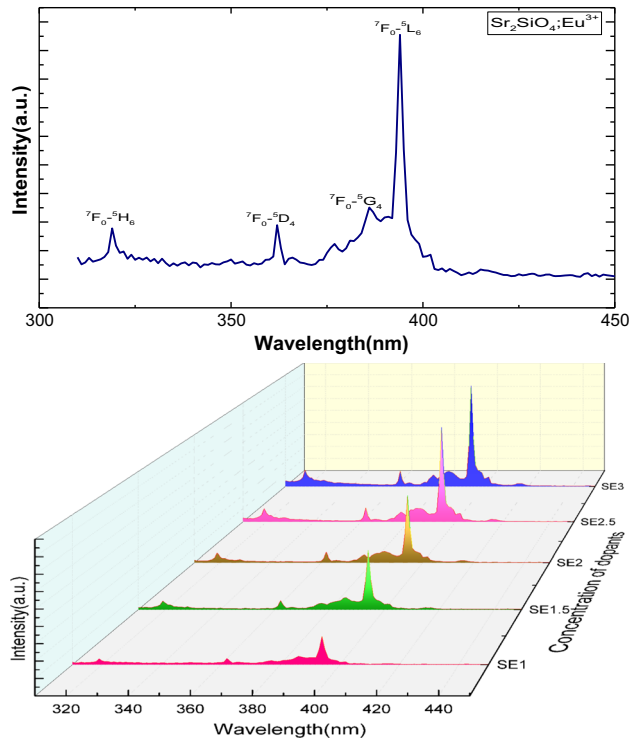


**Fig. 6** Concentration-dependent excitation spectra of  $\text{Sr}_2\text{SiO}_4:\text{Eu}^{3+}$  phosphors

between the ions of  $\text{Eu}^{3+}$ . Therefore, multipolar interaction was dominant mechanism for concentration quenching.

According to Dexter theory, when multipole–multipole interaction is involved in the energy transfer, variety of interactions such as dipole–dipole ( $d-d$ ), dipole–quadrupole ( $d-q$ ), and quadrupole–quadrupole ( $q-q$ ) interactions occur. The relation represented as Eq. (2) is exploited to determine the type of interaction involved in the energy transfer mechanism. The value of  $Q$  can be obtained by plotting  $\log(x)$  versus  $\log(I/x)$  as depicted in Fig. 8, where ‘ $x$ ’ is the activator concentration and  $I$  is the integral intensity of emission spectra. From the graph, the slope value was found to be 2.442. The value of  $Q$  was found to be 7.32, which is close to 8 which indicates that concentration quenching for the  $\text{Eu}^{3+}$  is caused by the energy transfer among the  $q-q$  interaction in  $\text{Sr}_2\text{SiO}_4:\text{Eu}^{3+}$  phosphor [21].

$$\frac{I}{x} = k \left[ 1 + \beta(x)^{\frac{Q}{3}} \right]^{-1} \quad (2)$$

where ‘ $I$ ’ is emission intensity per activator ion. Energy transfer behavior is widely existent in the rare-earth-ion-doped luminescence materials. The nature of energy transfer is decided by the microscopic physical mechanisms of the interactions between luminescent centers.

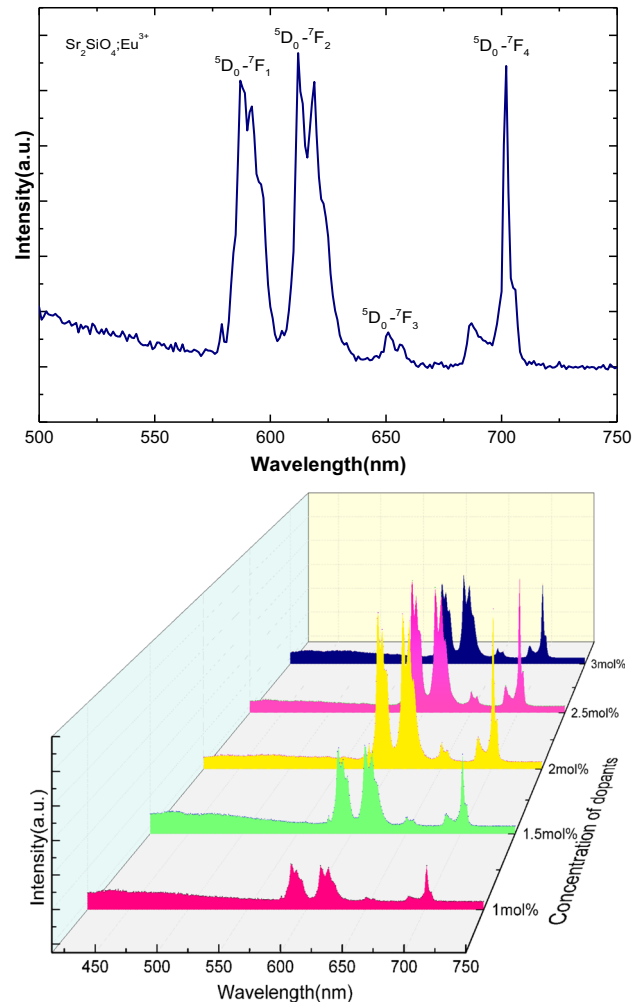


**Fig. 7** Concentration-dependent emission spectrum of  $\text{Sr}_2\text{SiO}_4:\text{Eu}^{3+}$  phosphors

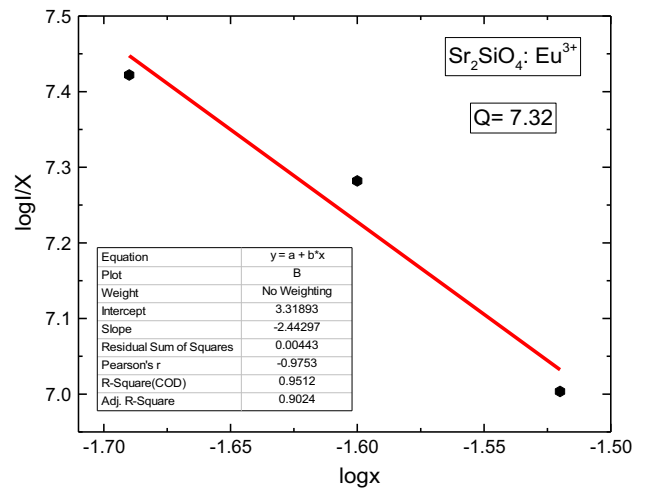


**Fig. 8**  $\log(x)$  versus  $\log(I/x)$ , for energy transfer mechanism to determine concentration quenching

### 3.6. CIE (Commission International de l'Eclairage) coordinates

The color coordinates are established by Commission International de l'Eclairage (CIE) in 1931 based on a two-dimensional graphical representation of any color perceptible by the human eye. The CIE coordinates could be obtained through commercial software by converting the data of photoluminescence emission spectrum. The CIE coordinates for the photoluminescence emission spectral data of  $\text{Sr}_{2-x}\text{Eu}_x\text{SiO}_4$  ( $\text{Sr}_2\text{SiO}_4:\text{Eu}^{3+}$ ) [ $x = 0.01, 0.015, 0.02, 0.025, 0.03$ ] silicate phosphors were calculated and are summarized in Table 2. The CIE chromatic diagram of  $\text{Eu}^{3+}$ -doped strontium silicate excited at wavelength 394 nm is shown in Fig. 9. The value of CIE coordinates

**Table 2** CIE coordinates for  $\text{Sr}_{2-x}\text{Eu}_x\text{SiO}_4$  [ $x = 0.01, 0.015, 0.02, 0.025, 0.03$ ] silicate phosphors

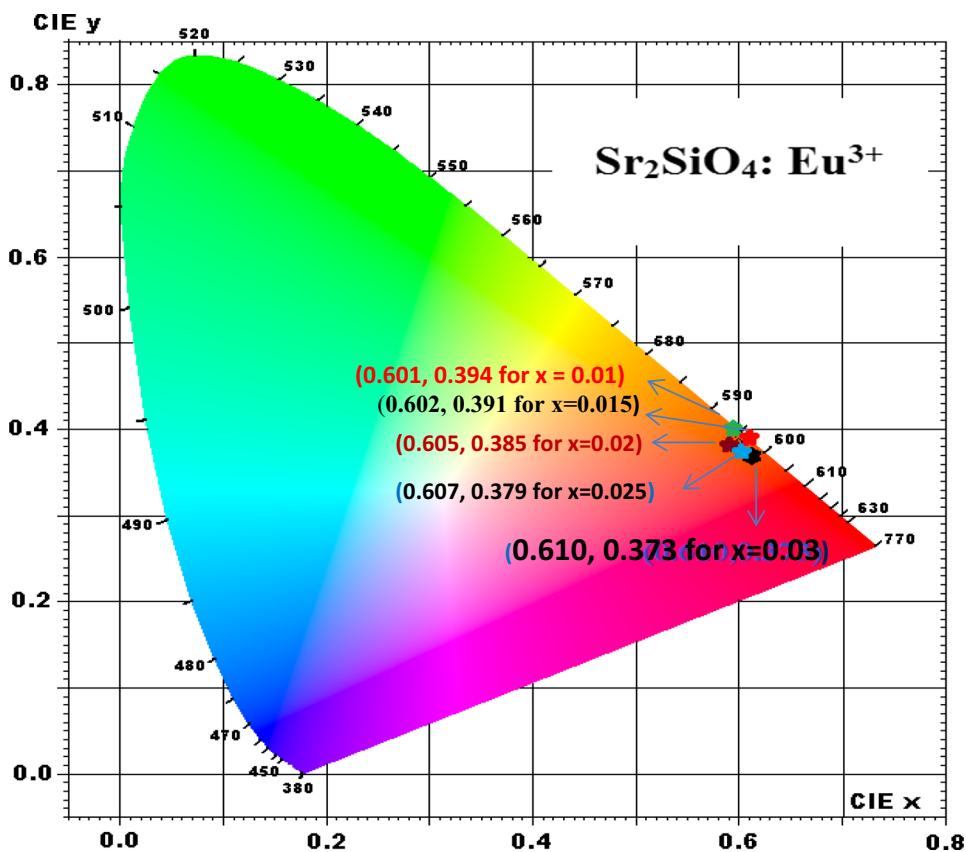
S. no.	Sample name	CIE coordinates (x, y)
1	$\text{Sr}_{1.99}\text{Eu}_{0.01}\text{SiO}_4$	(x = 0.601, y = 0.394)
2	$\text{Sr}_{1.985}\text{Eu}_{0.015}\text{SiO}_4$	(x = 0.603, y = 0.391)
3	$\text{Sr}_{1.98}\text{Eu}_{0.02}\text{SiO}_4$	(x = 0.605, y = 0.385)
4	$\text{Sr}_{1.975}\text{Eu}_{0.025}\text{SiO}_4$	(x = 0.607, y = 0.379)
5	$\text{Sr}_{1.97}\text{Eu}_{0.03}\text{SiO}_4$	(x = 0.610, y = 0.373)

corresponds to strong-red region and is consistent with the results reported elsewhere [22].

### 4. Conclusion

In the present study,  $\text{Sr}_{2-x}\text{Eu}_x\text{SiO}_4$  [ $x = 0.01, 0.015, 0.02, 0.025, 0.03$ ] silicate phosphors were successfully synthesized by high-temperature solid-state reaction method. The XRD and Rietveld refinement confirmed single phase with orthorhombic structure for the as-prepared phosphors. The optical band gap was calculated from UV-Vis diffuse reflectance spectroscopy that showed a trend of increase with increase in the  $\text{Eu}^{3+}$  concentration up to the  $x = 0.02$  after which band gap gradually decreases indicative of the maximum emission corresponding to this  $\text{Eu}^{3+}$  concentration. For the excitation at 394 nm, the  $\text{Sr}_2\text{SiO}_4:\text{Eu}^{3+}$  phosphors emitted orange red light displayed as emission peaks at 587 nm, 612 nm, and 702 nm corresponding to the transitions  $^5\text{D}_0 \rightarrow ^7\text{F}_0$ ,  $^5\text{D}_0 \rightarrow ^7\text{F}_1$ , and  $^5\text{D}_0 \rightarrow ^7\text{F}_4$  of  $\text{Eu}^{3+}$ , respectively. The maximum emission corresponding to  $x = 0.02$  is witnessed by the higher band gap estimated via UV-Vis spectral analysis. The PL emission in the orange red region has been confirmed from the calculated CIE coordinates.

**Fig. 9** CIE chromaticity diagram of  $\text{Sr}_{2-x}\text{Eu}_x\text{SiO}_4$  [ $x = 0.01, 0.015, 0.02, 0.025, 0.03$ ] phosphors



**Acknowledgements** UGC-DAE-CSR, Indore (M.P.), is highly acknowledged as an institute for extending characterization facilities. We are also thankful to Dr. V. Ganeshan, center director. Special thanks go to Dr. M. Gupta and Dr. U. P. Deshpande for the X-ray diffraction characterization and UV-Vis spectroscopy and guidance. Authors express gratitude to Dr. Srinibas Satapthy scientific officer laser material section, RRCAT, Indore (M.P.), for PL characterization and also thank Dr. P. Sharma School of Chemistry, DAVV, Indore, for FTIR characterization.

## References

- [1] R Ye, Z Cui, Y Hua, D Deng, S Zhao, C Li and S Xu *J. Non-Cryst. Solids* **357** 22 (2011)
- [2] W J Yang and T M Chen *Appl. Phys. Lett.* **88** 101 (2006)
- [3] J S Kim, P E Jeon and Y H Park, *Appl. Phys. Lett.* **85** 36 (2004)
- [4] T Stefan, P Peter, R Gundula, T Walter, K Wolfgang and S Detlef (2001) Light source comprising a light-emitting element. US Patent No. 6809347
- [5] J S Kim, Y H Park, J C Choi and H L Park *J. Electrochem. Soc.* **152** 135(2005)
- [6] H He, R L Fu, X L Zhang, X F Song, X R Zhao and Z W Pan *J. Mater. Sci. Mater. Electron.* **20** 433 (2009)
- [7] H Guo, X F Wang, X B Zhang, Y F Tang, L X Chen and C G Ma *J. Electrochem. Soc.* **157** 310 (2010)
- [8] Q Yanmin, Z Xinbo, Y Xiao, C Yan and G Hai *J. Rare Earths* **27** 323 (2009)
- [9] T Wu, F Meng, Y Du, Y Tian, J Ma and Z Bai *J. Mater. Sci. Mater. Electron.* **28** 10645 (2017)
- [10] M Saleem and D Varshney *RSC Advances* **8** 1600 (2018)
- [11] M Saleem, A Mishra and D Varshney *J. Supercond. Nov. Magn.* (2018). <https://doi.org/10.1007/s10948-018-4865-7>
- [12] M Saleem, D Singh, A Mishra and D Varshney *Mater. Res. Express.* **6** 026304 (2019)
- [13] M Saleem, B Bhaghat and A Mishra *J Inorg Organomet Polym* (2019). <https://doi.org/10.1007/s10904-019-01169-1>
- [14] C Chang and D Mao *J. Alloys Compd.* **390** 134 (2005)
- [15] G T Chandrappa, S Ghosh and K C Patil *J. Mater. Syn. Process* **72** 73 (1999)
- [16] R Chrysafi, T Perraki and G Kakali *J. Eur. Ceram. Soc.*, **27** 170 (2007)
- [17] J Tauc *Optical properties of solid's* F Abeles (ed.) (Amsterdam: North Holland Publishers) (1970)
- [18] B S Pratibha, M S Chandrashekhara, H Nagabhushana, K P Ramesh, B M Nagabhushana and C Hanumanthrayappa *Procedia Materials Science* **5** 944 (2014)
- [19] I M Nagpure, S Shah and S J Dhoble *J. Lumin.***129** (9) 898 (2009).
- [20] G Blass and B C Grabmaier, *Luminescent Materials* (Berlin: Springer) p 99 (1994)
- [21] B V Rao, K Jang, H S Lee, S S Yi and J H Jeong *J. Alloys Compd.* **496** 251 (2010)
- [22] D B Chaudhari, P Z Zambare and O H Mahajan *J. Appl. Phys* **9** (4) 37 (2017)

**Publisher's Note** Springer Nature remains neutral with regard to jurisdictional claims in published maps and institutional affiliations.